

Supplementary text

Analysis of cell migration

Dye fluorescent (PKH26) labeled cells were delivered into the cerebral spinal fluid (CSF) to evaluate ALDH^{hi}SSC^{lo} cell migration within the parenchyma (Supplementary Fig. 3).

Donor cells survived and proliferated, generating cell clusters laterally in the spinal cord parenchyma attached to the meninges. A total of 20% of these cells had already migrated into the spinal cord parenchyma through the pia mater as early as 5–7 days after transplantation. Cell invasion was also observed at root exits. Cell clusters were situated preferentially near the blood vessels and were probably favored by the nutrient supply. Few cells were detected in the brain of recipient animals, particularly in the area directly adjacent to the ventricular system. Cell attachments on the spinal cord surface as well as the cell cluster formations were less frequent in wild-type mice. Only 2–3% of donor cells invaded the parenchyma of non-mutated mice within 7 days.

Analysis of SMN expression in transplanted SMA spinal cord

We demonstrated that SMN+7 (full-length) mRNA levels had increased in the laser capture motoneurons after transplantation (2.1 fold, $P = 0.01$, treated SMA vs untreated SMA) (Supplementary Fig. 8). Western blot analysis of protein isolated from whole spinal cord tissue of SMA mice revealed the presence of both the full-length SMN protein and the SMN Δ 7 protein, as previously described in these mice (4). The level of full-length SMN protein in SMA mice was at least 14-fold lower than in wt. No apparent change in the ratio of full-length to SMN Δ 7 protein was evident after transplantation in the whole spinal cord of SMA mice (Supplementary Fig. 8).

Analysis of Cdkn1a and Hsbp1 protein levels in primary spinal motoneurons (PMNs) from SMA mice

We evaluated the expression of Cdkn1a and Hsbp1 proteins in SMA PNMs before and after coculture with ALDH^{hi}SSC^{lo} cells (Fig 9s c, d). We demonstrated that isolated PMNs from SMA expressed higher levels of Cdkn1a compared to wt (1.6 fold, $P = 0.007$, SMA vs wt). No difference was observed in Hsbp1 protein levels. The protein level was not modified by the coculture system.

Supplementary Figures

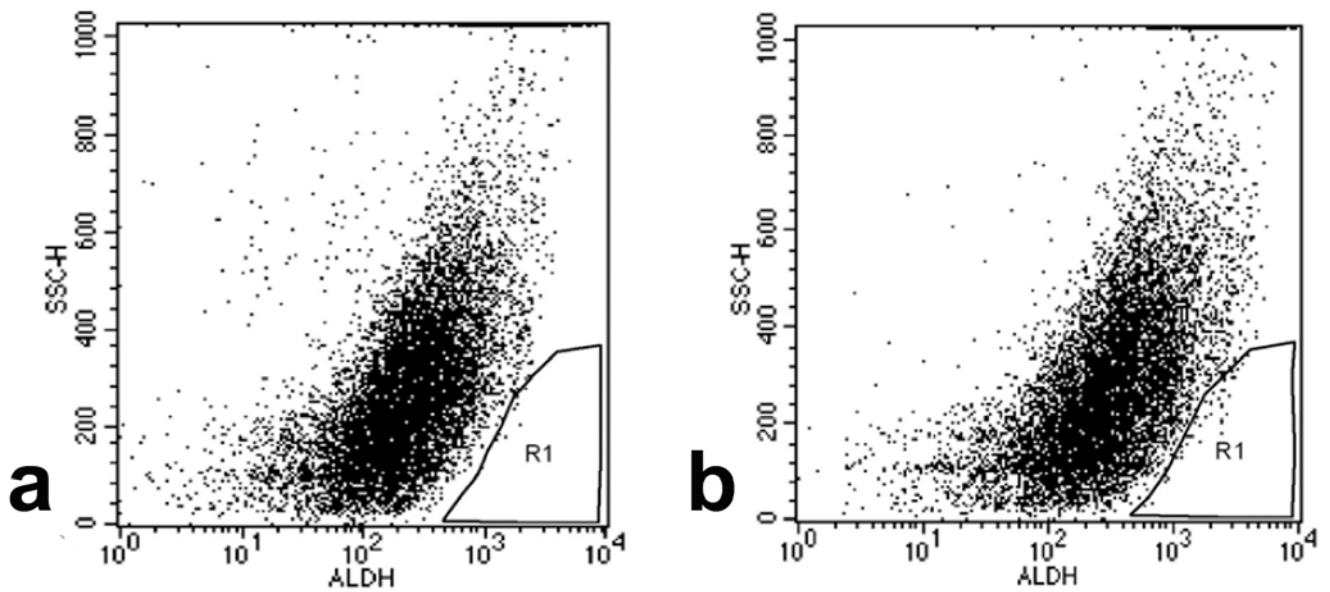


Figure 1 s

Identification, isolation, and differentiation of ALDH^{hi} SSC^{lo} cells into motoneuron-like cells.

(a, b) Flow cytometric analysis of ALDH activity on spinal-cord-derived NSCs. ALDH^{hi} SSC^{lo} cells were selected based on forward scatter (FSC) and side scatter (SSC) characteristics. NSCs incubated with Aldefluor substrate and the specific inhibitor of ALDH, diethylaminobenzaldehyde (DEAB), were used to establish the baseline fluorescence of these cells and to define the ALDH^{hi} region (a). Incubation of NSCs with Aldefluor substrate in the absence of an inhibitor induced a shift in FL1 fluorescence, defining the ALDH^{hi} population (b).

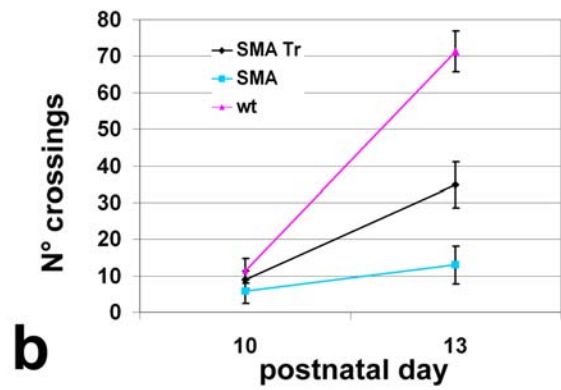


Figure 2 s

Neuromuscular evaluation of SMA mice.

(a) Photograph of hand grip assay of a treated SMA mouse. (b) Number of crossings in the open-field test in treated SMA mice (SMA Tr) and in untreated (SMA) and wild-type mice (wt). At 13 days of age, the number of crossings made by treated mice was significantly different from that of untreated mice ($P < 0.00001$).

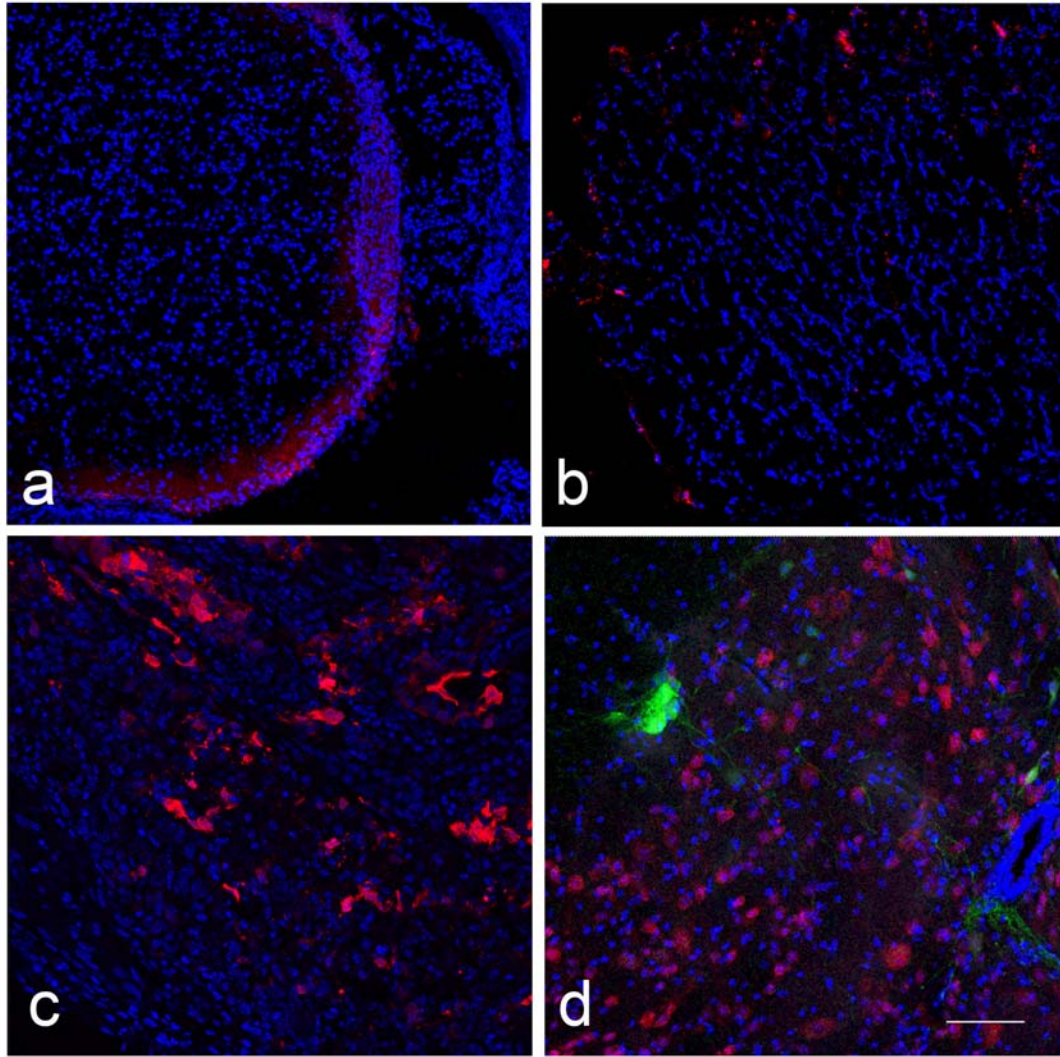


Figure 3 s

ALDH^{hi}SSC^{lo} cell migration into the spinal cord after intrathecal delivery.

Dye fluorescent (PKH26, red signal)-labeled cells were delivered into the CSF to evaluate ALDH^{hi}SSC^{lo} cell migration into the parenchyma. Five days after transplantation (**a**), donor cells were located laterally in the spinal cord parenchyma attached to the meninges, initiating through the pia mater in the parenchyma. After 7 (**b**) and 10 days (**c**), donor cells were observed in the parenchyma in gray and white matter. At the end of the disease, HB9-GFP neurons were detected in the ventral horn of transplanted mice (**d**). In panel (**d**), neurons are stained for the neuronal antigen NeuN (red signal). Scale bar: **a**: 300 μ m; **b-d**: 100 μ m.

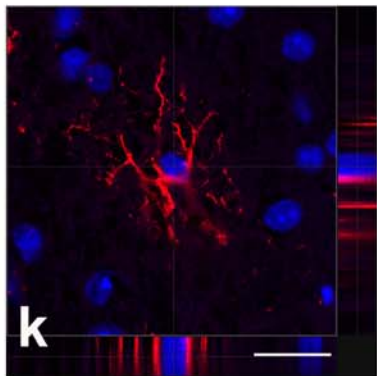
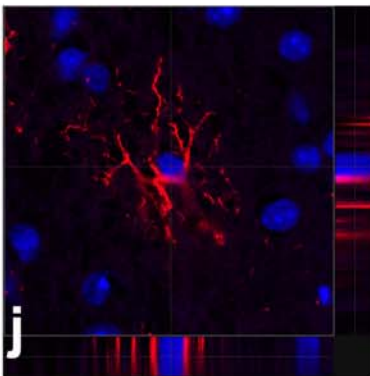
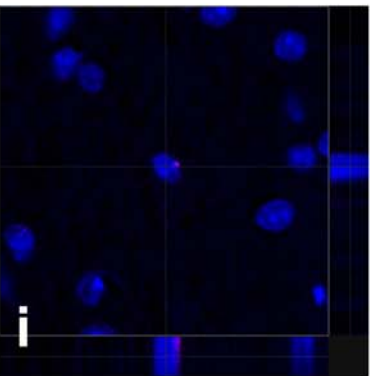
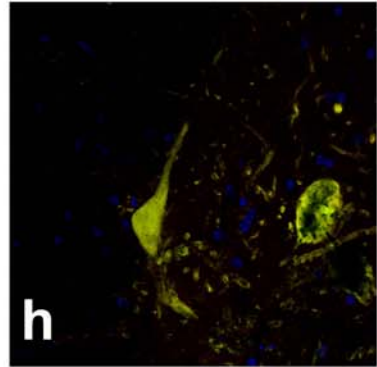
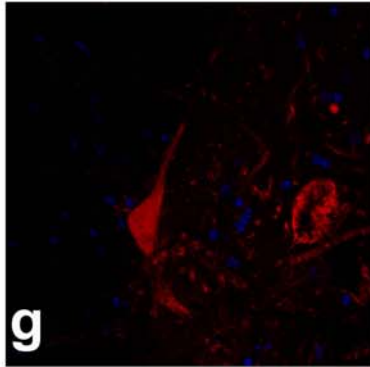
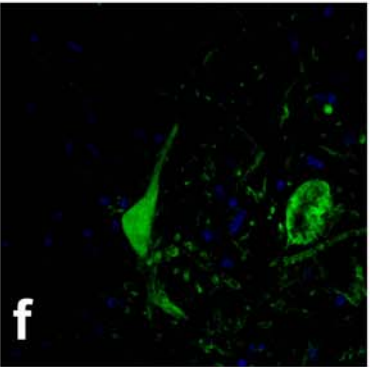
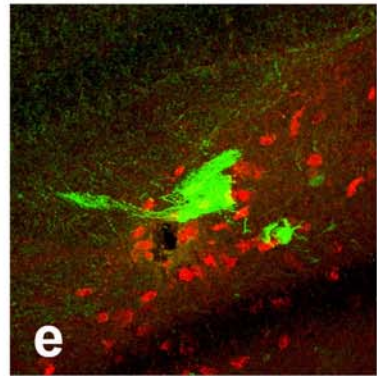
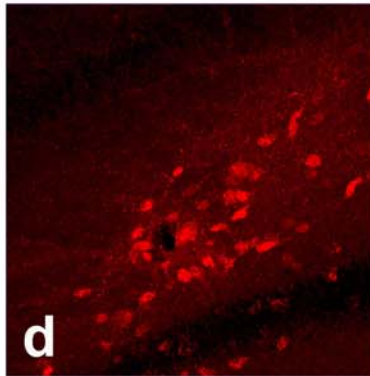
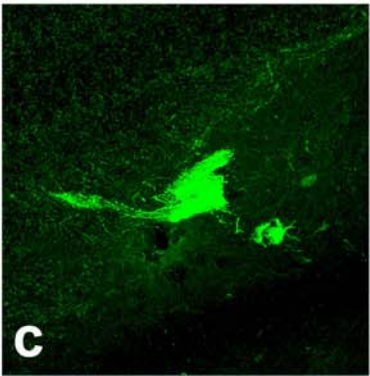
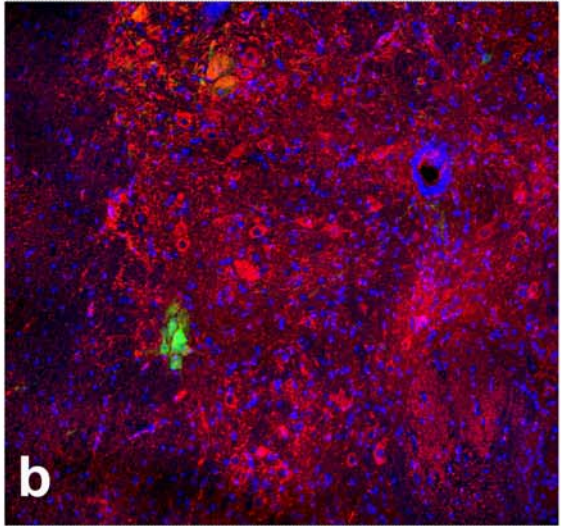
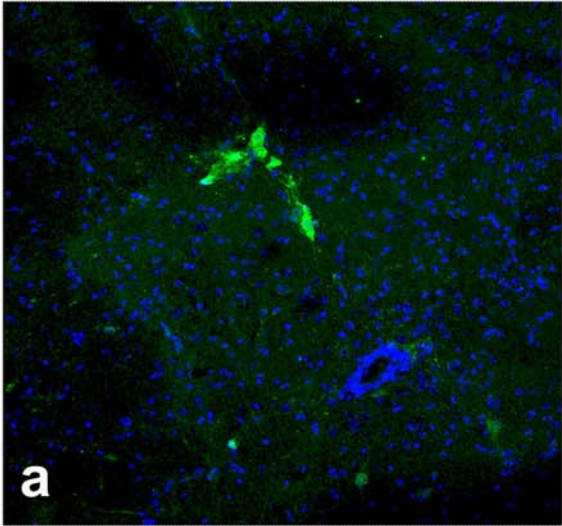


Figure 4 s

ALDH^{hi}SSC^{lo} cells transplanted into SMA mice engraft the host spinal cord.

ALDH^{hi}SSC^{lo} cells derived from HB9-GFP mice were transplanted intrathecally in P1 SMA mice. GFP⁺ neurons were detected in the anterior horn of the spinal cord, as shown in spinal cord coronal sections (**a**, **b**). Immunohistochemistry for neuroectodermal markers confirmed that these cells are differentiated into neurons. Confocal microscopy showed that GFP donor-derived neurons co-express neuronal specific proteins such as NF (**b**) and NeuN (**c–e**). (**f–h**) GFP cells present motoneuronal characteristics, as demonstrated by double immunofluorescence staining of GFP (green) under the HB9-specific motoneuronal promoter and cholinergic neurotransmitter (**f**: GFP; **g**: ChAT; **h**: merge). FISH analysis for Y chromosome in sex-mismatched transplantation experiments (male donor cells into a female recipient) permit the detection of other non-neuronal fates undertaken by transplanted cells such as astrocytes, as shown in **i–k**. **i**: Y chromosome (pink dot); **f**: GFAP (red signal); **k**: merge. Scale bars: **a–b**: 300 μ m; **i–k**: 75 μ m.

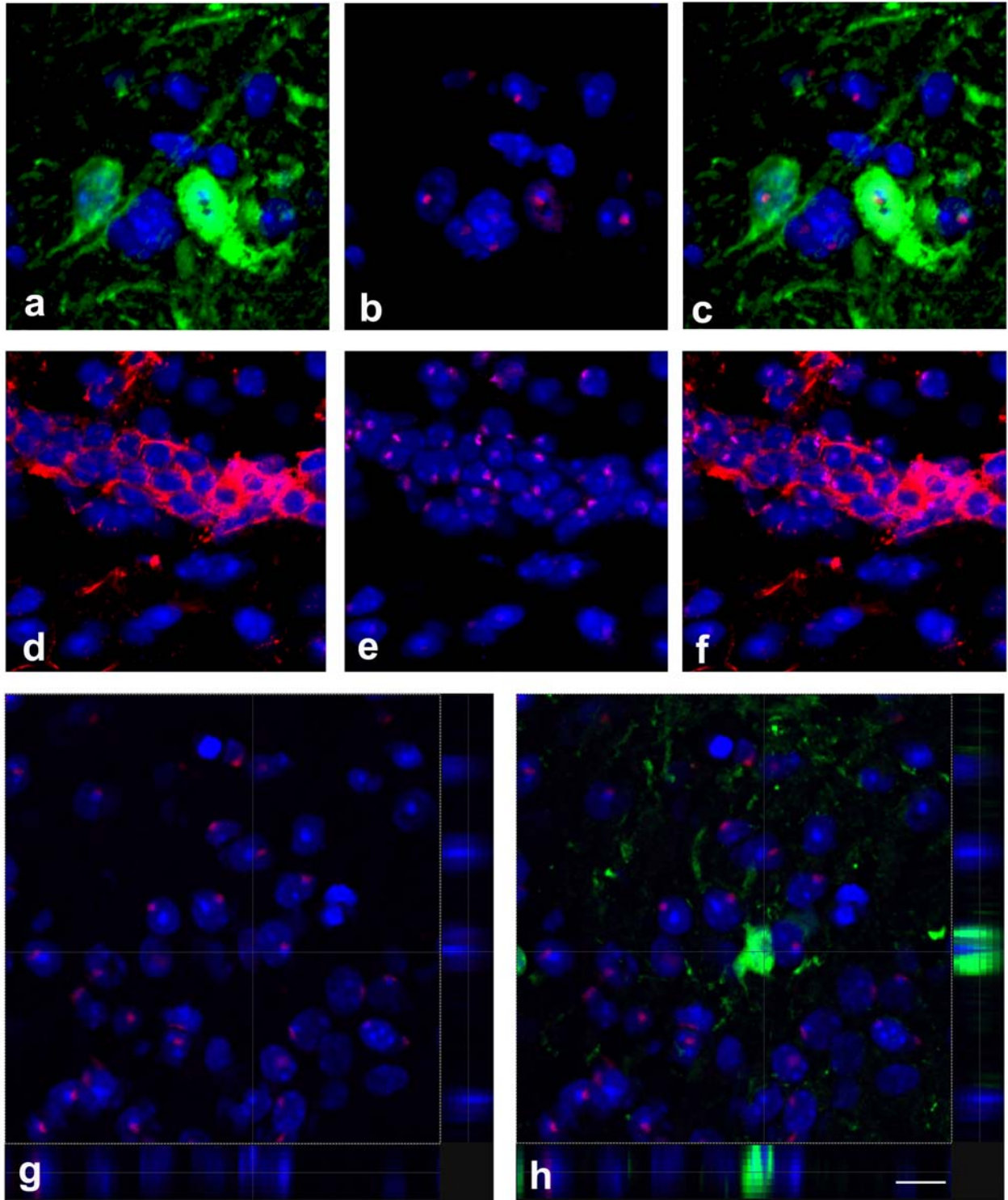


Figure 5 s

FISH analysis of SMA-transplanted spinal cord

a–f: FISH analysis for Y chromosome (dot signal) in sex-mismatched transplantation experiments (male donor cells into a female recipient) allows confirmation of the donor origin of HB9-GFP cells

(a–c), as well as detection of other phenotypes, such as donor neural stem/precursor cells, positive for nestin and Y chromosome, as shown in **d–f**.

(a–c) Two HB9-GFP neurons (green, **a**) presenting Y-positive signal (red dots, **b**) surrounded by other male donor cells (Y-positive red dots, **b**) and female host cells (negative for red signals, **b**). **(c)**: merge. **d–f**: Donor neural stem/precursor cells, positive for nestin (red, **d**) and Y chromosome (purple, **e**). **(f)**: merge.

g–h: FISH analysis for Y chromosome in male SMA mouse spinal cord recipients transplanted with donor female Hb9 cells permits exclusion of cell fusion events as shown in panels **g–i** in which a three-dimensional confocal reconstruction demonstrates an HB9-derived neuron that does not express the Y chromosome signal, surrounded by Y-positive male host cells (**g**: blue DAPI-stained nuclei with FISH red dot signals; **h**: merge with GFP). Scale bar: **a–c**: 35 μm ; **d–f**: 50 μm ; **g–h**: 50 μm .

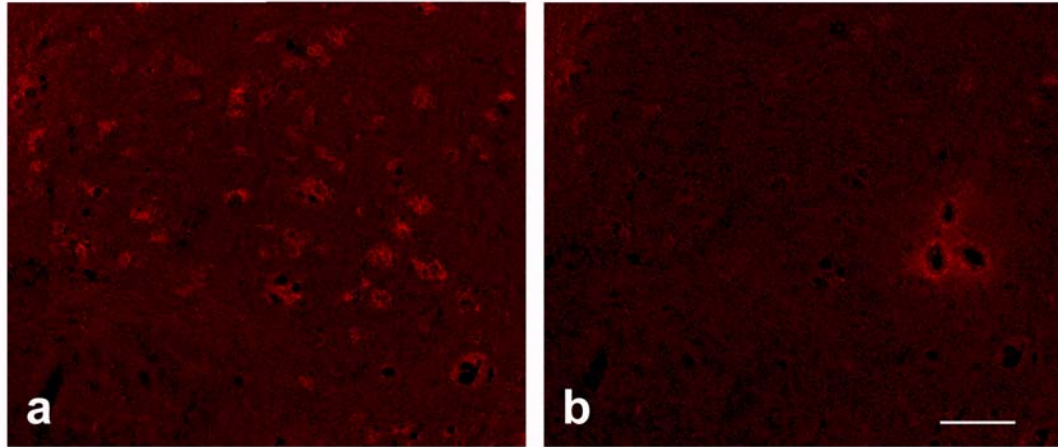


Figure 6 s

Laser capture microdissection (LCM) of endogenous SMA motoneurons

(**a, b**) Motoneuron cells stained for ChAT before (**a**) and after microdissection (**b**). Scale bar: 70 μm .

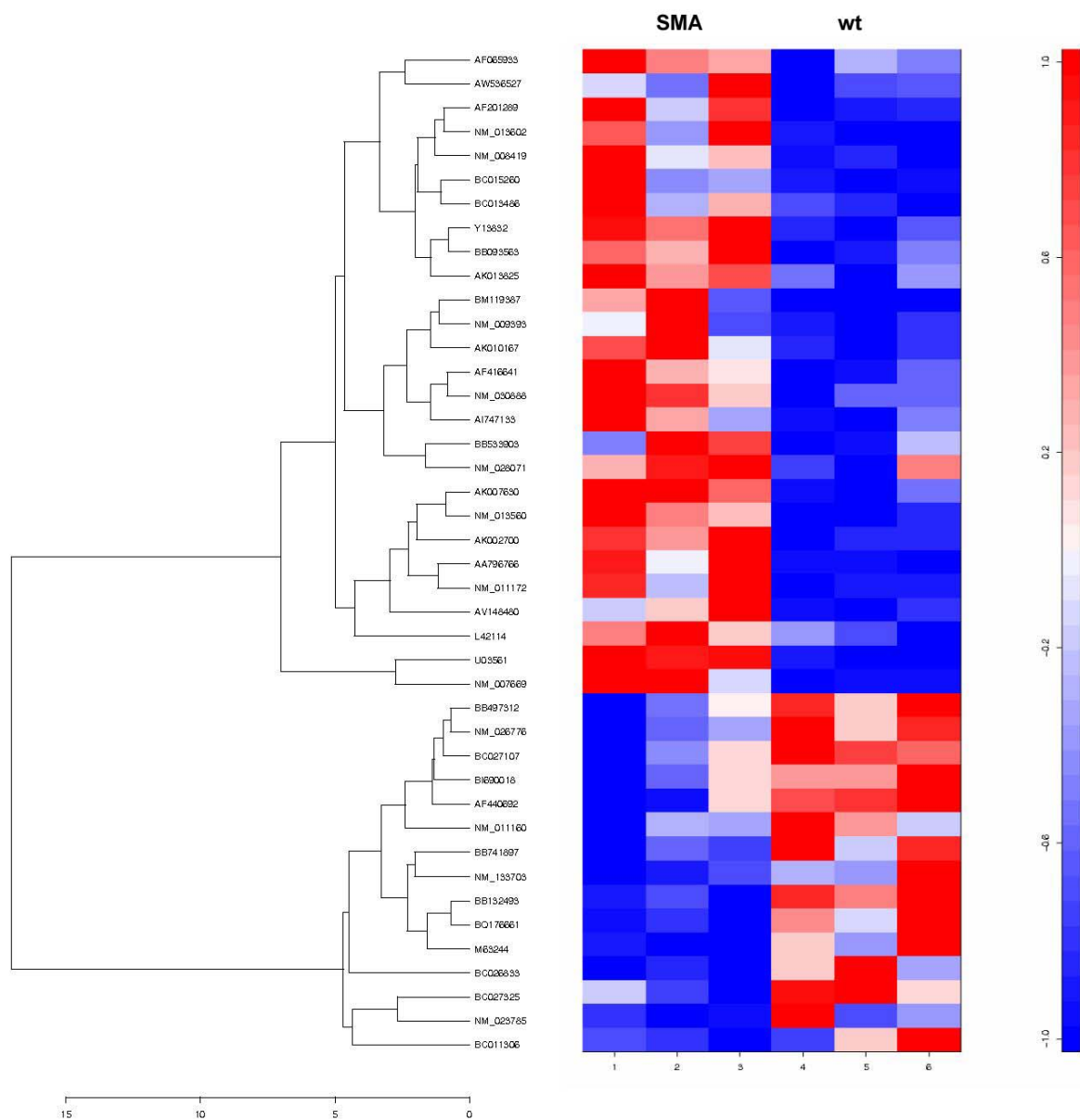


Figure 7 s

Cluster analysis of the differentially expressed genes in the comparison between SMA untreated and wt motoneurons.

The hierarchical cluster clearly subdivides upregulated (red) and downregulated (blue) genes in both groups. Color scale helps to visualize internal similarity.

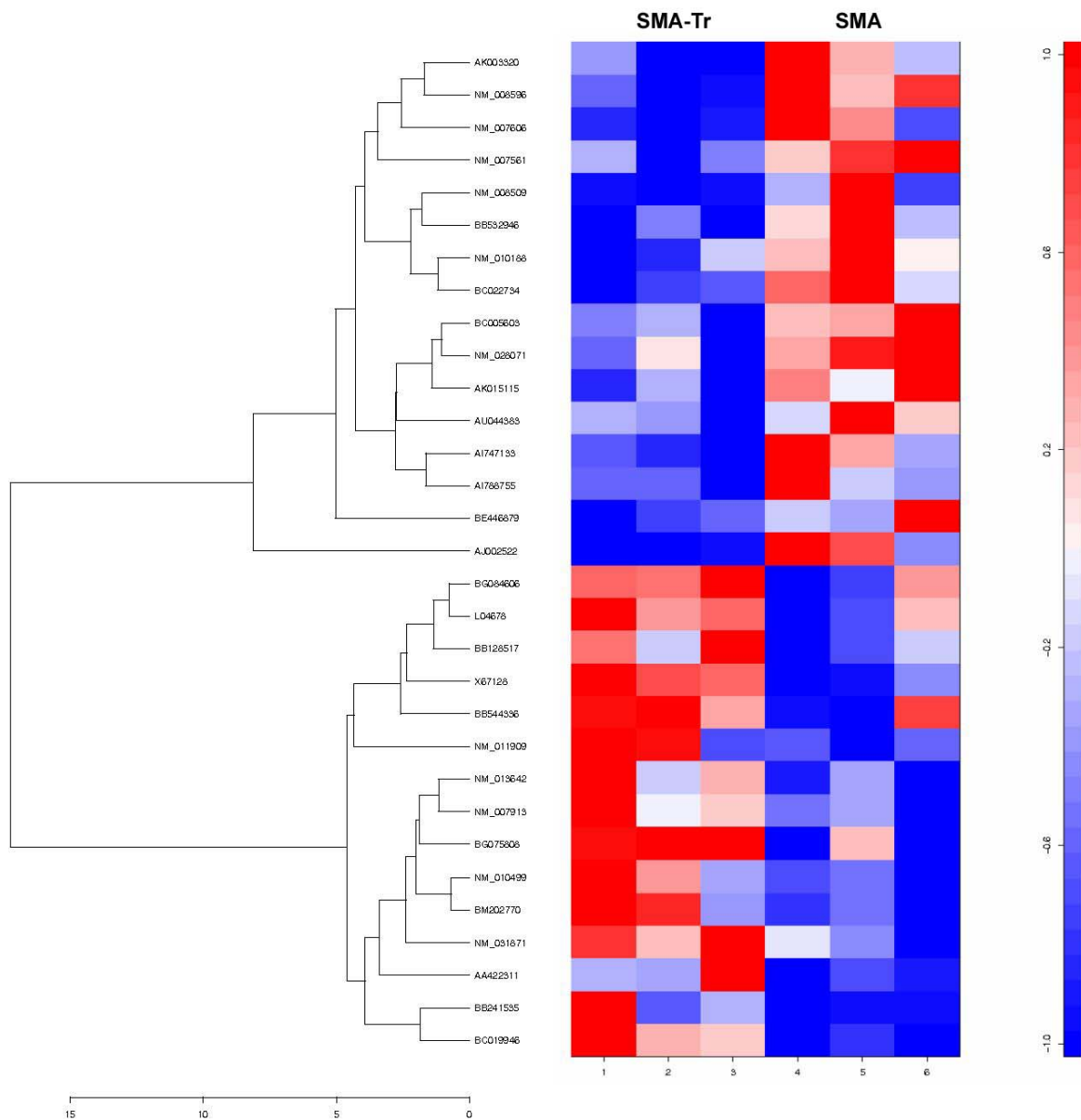


Figure 8 s

Cluster analysis of differentially expressed genes in the comparison between SMA treated and untreated motoneurons.

The hierarchical cluster subdivides upregulated (red) and downregulated (blue) genes in both groups. Color scale helps to visualize internal similarity.

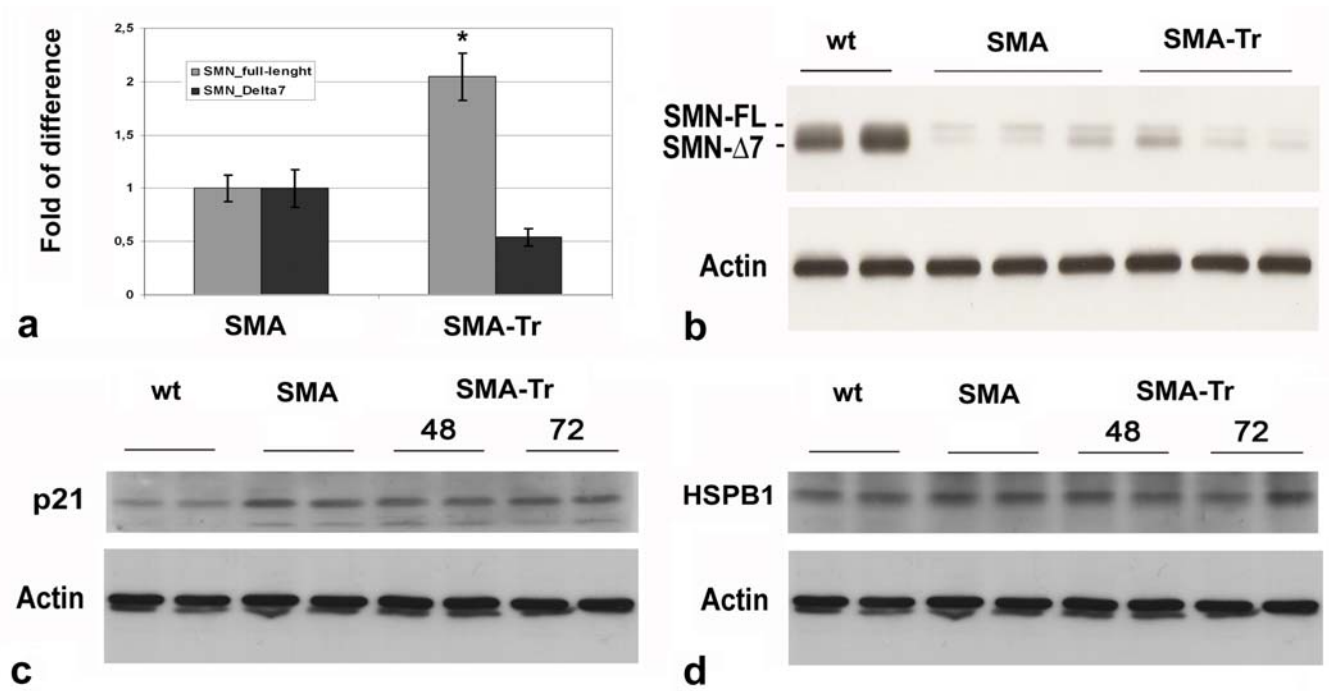


Figure 9 s

ALDH^{hi}SSC^{lo} cells increase expression of SMN.

(a) Transplanted ALDH^{hi}SSC^{lo} cells increase *SMN* full-length transcript in motoneurons (isolated by laser capture microdissection) *in vivo* (mean ± SD) (* $P < 0.02$ treated vs untreated). (b) Western blot analysis of the whole spinal cord of treated SMA mice did not show any increase in SMN protein levels. The upper bands show full-length SMN protein; the lower bands show SMNΔ7 protein. (c) Western blot analysis showed that isolated PMNs from SMA mice expressed a higher level of p21 compared to wt ($P = 0.007$, SMA vs wt) in line with results obtained by real-time PCR *in vivo*. The expression of *Cdkn1a* did not change after coculture. (d) No difference was observed in *Hspb1* protein levels before and after co-culture.

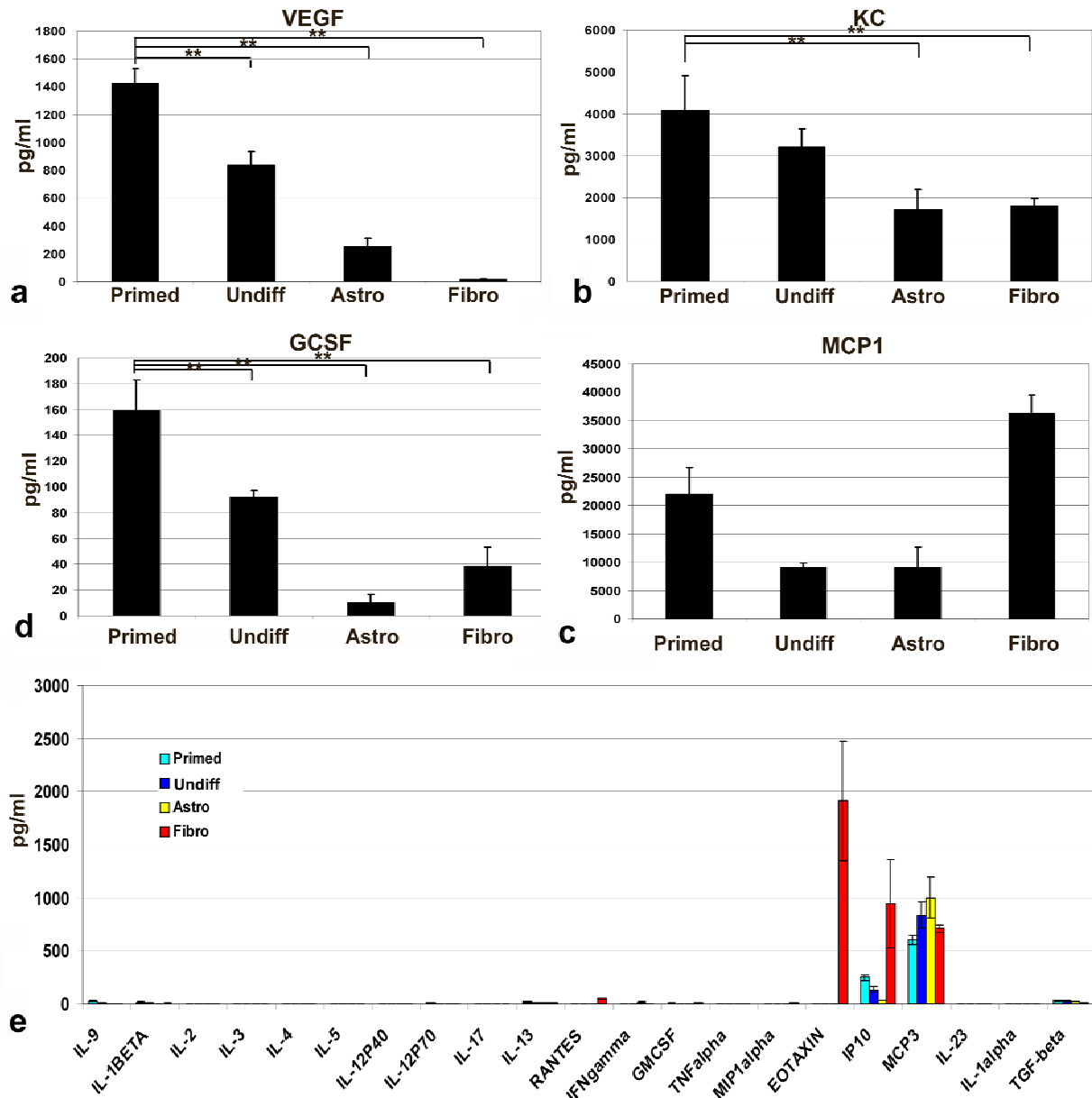


Figure 10 s

Cytokines profile

Luminex multi-analyte profiling (xMAP) technology was used to profile 26 cytokines in the cell supernatants of primed ALDH^{hi}SSC^{lo} NSCs, undifferentiated cells, astrocytes, and fibroblasts. **(a)** Primed ALDH^{hi}SSC^{lo}-derived cells expressed significantly higher levels of vascular endothelial growth factor (VEGF) (** P < 0.00001) compared to other cell types. **(b)** Primed ALDH^{hi}SSC^{lo} NSCs secreted significantly higher quantities of KC (CXCL1) than the other cell types (KC: primed vs undifferentiated, P = 0.02; primed vs astrocytes and primed vs fibroblasts, ** P < 0.00001,

respectively). (c) Granulocyte colony-stimulating factor (G-CSF) is produced by primed cells in a significantly higher quantity (G-CSF: primed vs other cells ** $P < 0.00001$). (d) All cell types analyzed expressed high MCP1 levels, with the highest level expressed by fibroblasts (MCP1: primed vs undifferentiated, $P = 0.000013$; primed vs astrocytes, $P = 0.000013$; primed vs fibroblasts, $P = 0.000027$). (e) Other proinflammatory cytokines were either not expressed or were secreted at very low levels in ALDH^{hi}SSC^{lo}-derived cells.

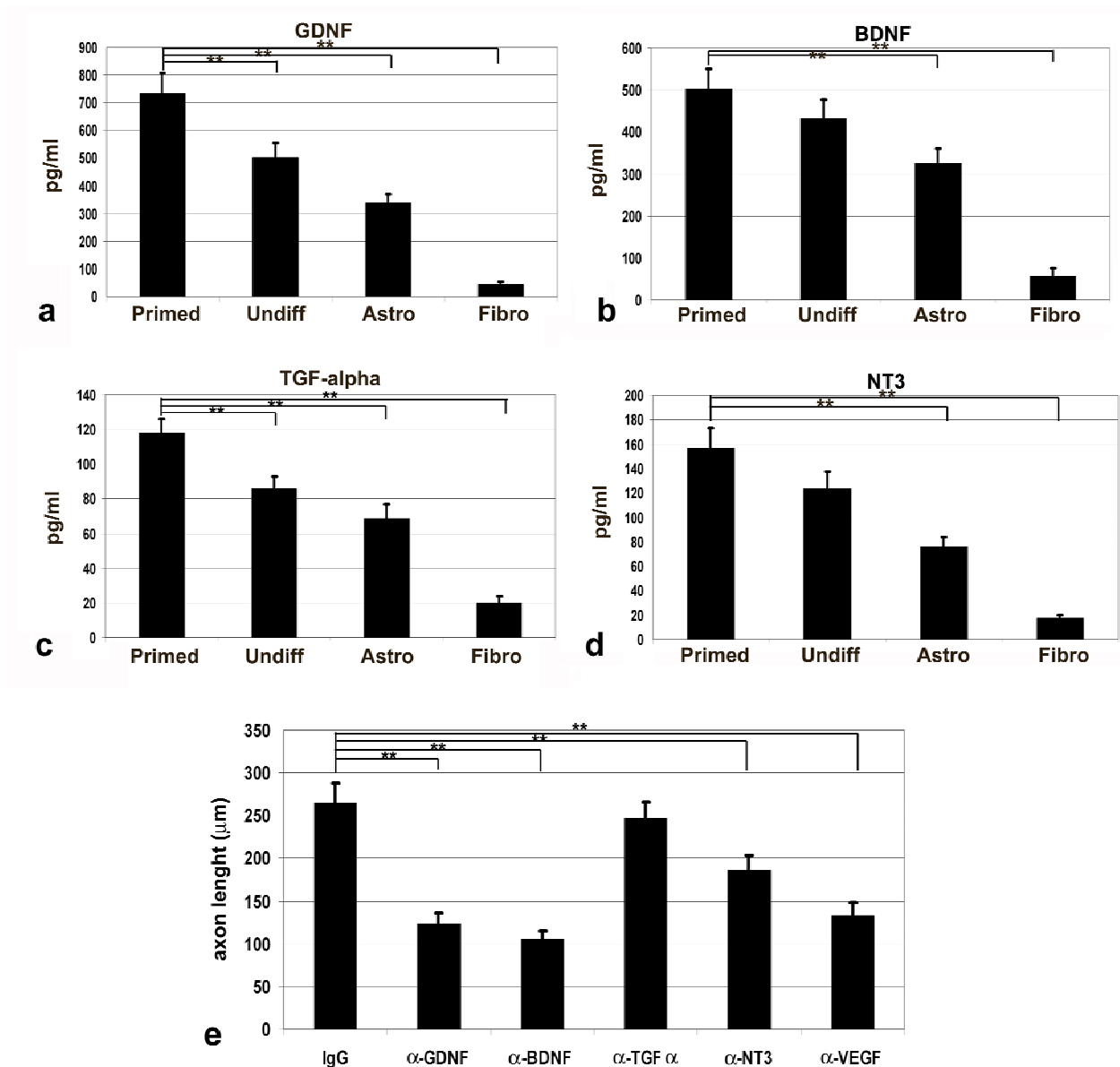


Figure 11 s

Primed ALDH^{hi}SSC^{lo} NSCs secrete neurotrophic factors

(a–d) ELISA assay was performed to detect the profile of neurotrophins (GDNF, BDNF, TGF- α , and NT-3). Primed ALDH^{hi}SSC^{lo} NSCs secrete significant amounts of GDNF (a) (primed vs other cells, ** $P < 0.00001$), BDNF (b) (primed vs undifferentiated, $P = 0.00013$; primed vs astrocytes and primed vs fibroblasts, ** $P < 0.00001$, respectively), TGF- α (c) (primed vs other cells, ** $P < 0.00001$), NT3 (d) (primed vs other cells, ** $P < 0.00001$). (e) The axonal growth of SMA PMNs

cocultured with primed ALDH^{hi}SSC^{lo} NSCs was inhibited by neutralizing antibodies for GDNF, BDNF, TGF- α , NT3, and VEGF compared to control antibody (IgG) (GDNF vs control, ** $P < 0.00001$; BDNF vs control, ** $P < 0.00001$; TGF- α vs control, ** $P = 0.00004$; NT3 vs control, ** $P < 0.00001$; VEGF vs control, ** $P < 0.00001$).

Tab. 1**Gene expression profile: untreated SMA mice vs wt**

Gene name	Accession number	Gene definition	Probe Affymetrix	Biological function	Ratio SMA/WT	Ratio Treated/SMA	Ratio Treated/WT
<i>Down-regulated genes</i>							
Gjb1	BC026833	gap junction membrane channel protein beta 1	1448767_s_at	nervous system development	0.21	2.19	0.46
Rsad2	BB741897	radical S-adenosyl methionine domain containing 2	1421009_at	immune response	0.31	1.39	0.43
Mkrn1	BQ176661	makorin, ring finger protein, 1	1418435_at	transcription activity, cell cycle regulation	0.34	1.24	0.42
Pomt1	BC027325	protein-O-mannosyltransferase 1	1424284_at	protein amino acid O-linked glycosylation	0.35	1.74	0.61
2810453I06Rik	NM_133703	RIKEN cDNA 2810453I06 gene	1418389_at		0.36	0.89	0.32
Vps25	NM_026776	vacuolar protein sorting 25	1421050_at	regulation of transcription, DNA-dependent antigen processing and presentation of peptide antigen via MHC class I	0.39	2.15	0.84
H2-K1	BC011306	histocompatibility 2, K1, K region	1425336_x_at		0.4	1.30	0.52
Anln	BI690018	anillin, actin binding protein	1433543_at	cytokinesis	0.4	1.38	0.55
Trf	AF440692	transferrin	1425546_a_at	iron ion	0.41	1.71	0.70

Slc13a3	BB497312	solute carrier family 13 (sodium-dependent dicarboxylate transporter), member 3	1438377_x_at	transport sodium ion transport	0.42	2.10	0.88
Cxcl7	NM_023785	chemokine (C-X-C motif) ligand 7	1418480_at	immune response	0.42	1.40	0.59
Arpp21	BC027107	cyclic AMP-regulated phosphoprotein, 21	1424248_at	signal transduction	0.43	1.95	0.84
Prkg1	NM_011160	protein kinase, cGMP-dependent, type I	1449876_at	dendrite development	0.43	0.58	0.25
Cyp51	NM_020010	cytochrome P450, family 51	1422534_at	electron transport	0.44	1.05	0.46

Up-regulated genes

Hspb1	U03561	heat shock protein 1	1425964_x_at	protein folding	11.1	0.42	4.69
Tmsb10	AV148480	thymosin, beta 10	1455946_x_at	actin cytoskeleton organization and biogenesis	5.55	0.70	3.91
Sult1a1	AK002700	sulfotransferase family 1A, phenol-preferring, member 1	1427345_a_at	lipid metabolism	5.2	0.71	3.69
Prodh	NM_011172	proline dehydrogenase	1417629_at	proline metabolism	4.35	0.69	3.02
Hspb1	NM_013560	heat shock protein 1	1422943_a_at	protein folding	4.35	0.46	1.98
Cdkn1a	AK007630	cyclin-dependent kinase inhibitor 1A (P21)	1424638_at	regulation of progression through cell cycle	4	0.90	3.60
Gdf10	L42114	growth differentiation factor 10	1424007_at	transforming growth factor beta receptor	3.7	0.62	2.28

Mt2	AA796766	metallothionein 2	1428942_at	signaling pathway nitric oxide mediated signal transduction	3.57	0.73	2.62
Tcap	AK010167	titin-cap	1423145_a_at	sarcomere organization	3.12	0.59	1.85
Mt1	NM_013602	metallothionein 1	1422557_s_at	nitric oxide mediated signal transduction	2.94	0.74	2.18
Kcna5	NM_008419	potassium voltage-gated channel, shaker-related subfamily, member 5	1417680_at	potassium ion transport	2.94	0.53	1.55
Tsc22d3	AF201289	TSC22 domain family 3	1425281_a_at	regulation of transcription, DNA-dependent	2.77	0.91	2.52
Ccl2	AF065933	chemokine (C-C motif) ligand 2	1420380_at	inflammatory response	2.7	1.33	3.60
Ddx5	AW536527	DEAD (Asp-Glu-Ala-Asp) box polypeptide 5	1433809_at	RNA splicing	2.7	1.12	3.03
Hif3a	AF416641	hypoxia inducible factor 3, alpha subunit	1425428_at	response to hypoxia, regulation of transcription, DNA-dependent	2.27	0.80	1.81

Tab. 2**Gene expression profile: treated SMA mice vs untreated**

Gene name	Accession number	Gene definition	Probe Affymetrix	Biological function	Ratio SMA/WT	Ratio Treated/SMA	Ratio Treated/WT
<i>Up-regulated genes</i>							
Atf3	BC019946	activating transcription factor 3	1449363_at	regulation of transcription, DNA-dependent	2.94	4.11	12.07
Socs3	BB241535	suppressor of cytokine signaling 3	1455899_x_at	regulation of cell growth	1.16	4.03	4.66
Tcrb-J	X67128	T-cell receptor beta, joining region	1452205_x_at	cellular defense response	0.42	3.97	1.68
5430435G22Rik	BB128517	RIKEN cDNA 5430435G22 gene	1424987_at	small GTPase mediated signal transduction	0.33	2.81	0.93
Phka1	AA422311	phosphorylase kinase alpha 1	1422744_at	glycogen metabolism	0.44	2.73	1.21
Ier2	NM_010499	immediate early response 2	1416442_at	immediate-early gene inducible	1.04	2.53	2.64
Itgb4	L04678	integrin beta 4	1427387_a_at	cell-matrix adhesion	0.50	2.51	1.25
Dusp1	NM_013642	dual specificity phosphatase 1	1448830_at	response to oxidative stress	2.01	2.51	5.04
Ccdc46	BG075808	coiled-coil domain containing 46	1427205_x_at		1.22	2.50	3.04

Cyr61	BM202770	cysteine rich protein 61	1438133_a_at	regulation of cell growth	0.89	2.43	2.16
Ildr1	BG084606	immunoglobulin-like domain containing receptor 1	1423276_at	receptor activity	0.55	2.41	1.33
Usp18	NM_011909	ubiquitin specific peptidase 18	1418191_at	ubiquitin-dependent protein catabolism	0.95	2.36	2.25
Ghdc	NM_031871	GH3 domain containing	1419502_at	GTPase activator activity	0.70	2.35	1.64
Egr1	NM_007913	early growth response 1	1417065_at	regulation of transcription, DNA-dependent	1.30	2.33	3.04
Zdhhc14	BB544336	zinc finger, DHHC domain containing 14	1438151_x_at	zinc ion binding	0.58	2.31	1.35

Down-regulated genes

Myh1	AJ002522	myosin, heavy polypeptide 1, skeletal muscle, adult	1427868_x_at	cytoskeleton organization and biogenesis	1.88	0.08	0.15
Car3	NM_007606	carbonic anhydrase 3	1460256_at	one-carbon compound metabolism	4.53	0.30	1.36
Sypl2	NM_008596	synaptophysin-like 2	1449206_at	calcium ion homeostasis	3.32	0.31	1.03
Rbm5	BE446879	RNA binding motif	1438069_a_at	negative	1.59	0.32	0.51

		protein 5		regulation of progression through cell cycle morphogenesis			
Shroom3	AK003320	shroom family member 3	1454211_a_at	cell morphogenesis	1.81	0.32	0.58
4930408O21Rik	AK015115	RIKEN cDNA 4930408O21 gene	1431741_a_at		1.56	0.34	0.53
Bmpr2	NM_007561	bone morphogenic protein receptor, type II (serine/threonine kinase)	1419616_at	transforming growth factor beta receptor signaling pathway	0.58	0.36	0.21
Errfi1	AI788755	ERBB receptor feedback inhibitor 1	1419816_s_at	stress-activated protein kinase signaling pathway	1.35	0.37	0.50
Lpl	NM_008509	lipoprotein lipase	1415904_at	lipid metabolism	2.20	0.40	0.88
Capn6	AI747133	calpain 6	1450429_at	proteolysis	2.39	0.41	0.98
Taf11	BC005603	TAF11 RNA polymerase II, TATA box binding protein (TBP)-associated factor	1451995_at	regulation of transcription, DNA-dependent	1.02	0.41	0.42
Npl	BC022734	N-acetylneuraminatase	1424265_at	N-acetylneuraminatase lyase activity	2.14	0.42	0.90
Josd3	AU044383	Josephin domain containing 3	1452635_x_at		1.14	0.43	0.49
BC003993	BB532946	cDNA sequence	1438278_a_at	RNA binding	2.07	0.43	0.89

Tab. 3**List of genes involved in the RNA processing**

Gene Name	Accession Number	Gene definition	Probe Affymetrix	Ratio SMA/WT	Ratio Treated/SMA	Ratio Treated/WT
Hnrpk	BB722680	Heterogeneous nuclear ribonucleoprotein K	1454692_x_at	2.00	0.7	1.40
Fus	AF224264	fusion, derived from t(12;16) malignant liposarcoma (human)	1451285_at	1.72	0.53	0.91
Dhx9	U91922	DEAH (Asp-Glu-Ala-His) box polypeptide 9	1425617_at	1.64	0.81	1.33
Rbm5	BE446879	RNA binding motif protein 5	1438069_a_at	1.59	0.32	0.51
Snrpd3	AK019453	small nuclear ribonucleoprotein D3	1422885_at	1.49	0.76	1.13
Snrp70	BC002169	U1 small nuclear ribonucleoprotein polypeptide A	1451104_a_at	1.43	0.63	0.90
Sfpq	BF224766	splicing factor proline/glutamine rich (polypyrimidine tract binding protein associated)	1438459_x_at	1.43	0.68	0.97
Trnt1	BM225164	tRNA nucleotidyl transferase, CCA-adding, 1	1425562_s_at	1.41	0.73	1.03
Sf1	BC009091	Splicing factor 1	1423750_a_at	1.39	0.8	1.11
Trit1	BC019812	tRNA isopentenyltransferase 1	1424489_a_at	1.35	0.79	1.07
Hnrpa2b1	C88150	heterogeneous nuclear ribonucleoprotein A2/B1	1433829_a_at	1.33	0.44	0.59
Prpf4b	BC003769	PRP4 pre-mRNA processing factor 4 homolog B (yeast)	1451909_a_at	1.33	0.77	1.03
Sfrs7	BE825013	splicing factor, arginine/serine-rich 7	1436871_at	1.30	0.8	1.04
Dhx9	U91922	DEAH (Asp-Glu-Ala-His) box polypeptide 9	1451770_s_at	1.30	0.75	0.97
Xab2	NM_026156	XPA binding protein 2	1448278_at	1.30	0.73	0.95
Srrm1	NM_016799	serine/arginine repetitive matrix 1	1450045_at	1.28	0.77	0.99
Sf3a3	AK015776	splicing factor 3a, subunit 3	1432488_a_at	1.28	0.52	0.67
Sf3a3	BC009141	splicing factor 3a, subunit 3	1423811_at	1.27	0.78	0.99

Sf3a1	BB031756	splicing factor 3a, subunit 1	1449333_at	1.25	0.75	0.94
Fus	AF224264	fusion, derived from t(12;16) malignant liposarcoma (human)	1451286_s_at	1.25	0.77	0.96
Cugbp1	AK014492	CUG triplet repeat, RNA binding protein 1	1427413_a_at	1.25	0.75	0.94
Fusip1	AF060490	FUS interacting protein (serine-arginine rich) 1	1423982_at	1.25	0.76	0.95
Rpp30	BG069849	ribonuclease P/MRP 30 subunit (human)	1423373_at	0.83	1.16	0.96
Hnrpr	BB822465	heterogeneous nuclear ribonucleoprotein R	1452030_a_at	0.81	1.3	1.06
Snrpa	NM_015782	small nuclear ribonucleoprotein polypeptide A	1417274_at	0.81	1.32	1.07
Ddx56	BC018291	DEAD (Asp-Glu-Ala-Asp) box polypeptide 56	1423815_at	0.81	1.28	1.03
Snrpn	NM_013670	small nuclear ribonucleoprotein N	1415895_at	0.81	1.39	1.12
Crnkl1	NM_025820	Crn, crooked neck-like 1 (Drosophila)	1420849_at	0.80	1.48	1.18
Hnrpab	BB168316	heterogeneous nuclear ribonucleoprotein A/B	1455855_x_at	0.80	1.23	0.98
Fbl	NM_007991	fibrillarin	1416684_at	0.80	1.42	1.14
Snrpn	NM_013670	small nuclear ribonucleoprotein N	1415896_x_at	0.79	1.23	0.98
0610009D07Rik	BE199670	RIKEN cDNA 0610009D07 gene	1436681_x_at	0.76	1.21	0.92
Fusip1	NM_010178	FUS interacting protein (serine-arginine rich) 1	1449121_at	0.75	1.25	0.94
EG666609	NM_026506	small nuclear ribonucleoprotein polypeptide G	1448357_at	0.75	1.32	0.99
Bop1	BM213936	block of proliferation 1	1423264_at	0.73	1.33	0.97
Rbm8a	NM_025875	RNA binding motif protein 8a	1418120_at	0.72	1.46	1.05
Rpp14	BI455861	ribonuclease P 14 subunit (human)	1419461_at	0.67	1.31	0.88